

Bis(cyclopentadienyl)chromium and Bis(cyclopentadienylvanadium) Composites of Mesoporous Niobium Oxide with Pseudo-One-Dimensional Organometallic Wires in the Pores

Xun He,[†] Michel Trudeau,[‡] and David Antonelli^{*,†}

Department of Chemistry and Biochemistry, University of Windsor, 401 Sunset Avenue, Windsor, Ontario N9B-3P4, Canada, and Emerging Technologies, Hydro-Québec Research Institute, 1800 Boulevard Lionel-Boulet, Varennes, Québec, J3X 1S1, Canada

Received August 8, 2001. Revised Manuscript Received September 19, 2001

New composites of mesoporous niobium oxide with mixed oxidation state bis(cyclopentadienyl)vanadium and -chromium phases in the pores were synthesized and characterized by X-ray powder diffraction, nitrogen adsorption, UV, electron paramagnetic resonance (EPR), X-ray photoelectron spectroscopy (XPS), and superconducting quantum interference device magnetometry. The XPS and EPR revealed that the walls of the mesostructure in both composites were reduced and that the organometallic had retained its structural integrity as a combination of neutral and cationic metallocene species. The conductivity of these materials ranged from 10^{-4} to $10^{-6} \Omega^{-1} \text{ cm}^{-1}$ and was attributed to the mixed oxidation state organometallic phase since previous studies showed that the reduced niobium oxide mesostructure is inherently insulating. The Hubbard model involving the bandwidth and the Hubbard potential was invoked using electron affinities, ionization potentials, and bandwidths of the organometallic species to verify the model involving electron mobility through the mixed oxidation state organometallic phase. Comparisons to previously studied insulating cobaltocene composites of mesoporous niobium oxide were made in an effort to determine the main factors governing conductivity in these systems.

Introduction

Recently we showed that mesoporous niobium, titanium, and tantalum oxides^{1–5} could be reduced with up to 1 molar equiv of alkali-metal naphthalene reagent.^{6,7} This was the first example of a molecular sieve with a reducible framework and demonstrates that these materials^{8–11} have physical properties different from those of their electrochemically inert MCM-41 silica analogues.^{12–17} Because of the controllable porosity of

the reducible oxide framework and the potential to tune the oxidation state and electronic properties of the walls, these materials may find applications in the fabrication of a wide range of nanoelectronic devices where fast internal diffusion and tunable electronic properties are necessary.^{18–21} While the alkali-metal-reduced mesoporous niobium oxide materials are insulating due to localization of the electrons in energy wells or local defects, materials reduced with alkali-metal fullerenes^{22,23} display surprisingly high conductivities, attributable to

[†] University of Windsor.

[‡] Hydro-Québec Research Institute.

- (1) (a) Antonelli, D. M.; Ying, J. Y. *Angew. Chem., Int. Ed. Engl.* **1996**, *35*, 426. (b) Antonelli, D. M.; Nakahira, A.; Ying, J. Y. *Inorg. Chem.* **1996**, *35*, 3126.
 (2) Antonelli, D. M.; Ying, J. Y. *Chem. Mater.* **1996**, *8*, 874.
 (3) Antonelli, D. M. *Microporous Mesoporous Mater.* **1999**, *30*, 315.
 (4) Antonelli, D. M. *Microporous Mesoporous Mater.* **1999**, *33*, 209.
 (5) Antonelli, D. M.; Trudeau, M. *Angew. Chem., Int. Ed. Engl.* **1999**, *38*, 1471.
 (6) Vettraino, M.; Trudeau, M.; Antonelli, D. M. *Adv. Mater.* **2000**, *12*, 337.
 (7) Vettraino, M.; Trudeau, M.; Antonelli, D. M. *Inorg. Chem.* **2001**, *40*, 2088.
 (8) Tian, Z. R.; Wang, J. Y.; Duan, N. G.; Krishnan, V. V.; Suib, S. L. *Science* **1997**, *276*, 926.
 (9) Mamak, M.; Coombs, N.; Ozin, G. *Adv. Mater.* **2000**, *12*, 198.
 (10) Liu, P.; Liu, J.; Sayari, A. *Chem. Commun.* **1997**, 577.
 (11) Ciesla, U.; Demuth, D.; Leon, R.; Petroff, P.; Stucky, G.; Unger, K.; Schuth, F. *J. Chem. Soc., Chem. Commun.* **1994**, 1387.
 (12) (a) Kresge, C. T.; Leonowicz, M. E.; Roth, W. J.; Vartulli, J. C.; Beck, J. S. *Nature* **1992**, *359*, 710. (b) Beck, J. S.; Vartulli, J. C.; Roth, W. J.; Leonowicz, M. E.; Kresge, C. T.; Schmitt, K. D.; Chu, C. T.-W.; Olson, D. H.; Shepard, E. W.; McCullen, S. B.; Higgins, J. B.; Schlenker, J. L. *J. Am. Chem. Soc.* **1992**, *114*, 10834.

- (13) (a) Huo, Q.; Margolese, D. I.; Ciesla, U.; Demuth, D. G.; Feng, P.; Gier, T. E.; Sieger, P.; Firouzi, A.; Chmelka, B. F.; Schuth, F.; Stucky, G. D. *Chem. Mater.* **1994**, *6*, 1176. (b) Firouzi, A.; Kumar, D.; Bull, L. M.; Besier, T.; Sieger, P.; Huo, Q.; Walker, S. A.; Zasadzinski, J. A.; Glinka, C.; Nicol, J.; Margolese, D.; Stucky, G. D.; Chmelka, B. F. *Science* **1995**, *267*, 1138.
 (14) Chen, C.-Y.; Burkette, S. L.; Li, H.-X.; Davis, M. E. *Microporous Mater.* **1993**, *2*, 27.
 (15) Tanev, P. T.; Chibwe, M.; Pinnavaia, T. J. *Nature* **1994**, *368*, 321.
 (16) (a) Antonelli, D. M.; Ying, J. Y. *Curr. Opin. Colloid Interface Sci.* **1996**, *1*, 523. (b) Antonelli, D. M.; Ying, J. Y. *Angew. Chem., Int. Ed. Engl.* **1995**, *34*, 2014.
 (17) Behrens, P. *Angew. Chem., Int. Ed. Engl.* **1996**, *35*, 515.
 (18) Kopelman, R.; Parus, S. J.; Prasad, J. *Chem. Phys.* **1988**, *128*, 209.
 (19) Dozier, W. D.; Drake, J. M.; Klafter, J. *Phys. Rev. Lett.* **1986**, *56*, 197.
 (20) Wu, C.-G.; Bein, T. *Chem. Mater.* **1994**, *6*, 1109.
 (21) Wu, C. G.; Bein, T. *Science* **1994**, *264*, 1757.
 (22) Ye, B.; Trudeau, M.; Antonelli, D. M. *Adv. Mater.* **2001**, *13*, 29.
 (23) Ye, B.; Trudeau, M.; Antonelli, D. M. *Adv. Mater.* **2001**, *13*, 561.

the presence of one-dimensional fulleride phases within the insulating channels of the structure. Mesoporous niobium oxide reduced with cobaltocene is insulating and superparamagnetic,^{24,25} while the nickelocene analogues undergo an unusual superparamagnetic to spin glass transition.²⁶ In contrast, composites synthesized with bis(benzene)chromium²⁷ and bis(benzene)vanadium²⁸ are paramagnetic and semiconducting, with conductivity values as high as $10^{-4} \Omega^{-1}\text{cm}^{-1}$.

In this paper we compare the electronic behavior of new bis(cyclopentadienyl)vanadium and -chromium composites to that of previously studied bis(benzene)vanadium and -chromium composites to gauge the effect of changing from a zerovalent bis(arene) dopant to the corresponding isostructural divalent metallocene analogue. Since conductivity in solids depends on a balance between U , the Hubbard potential (the difference between the ionization potential and the electron affinity of the charge-carrying species in question) and the bandwidth, W , where electron mobility is favored when $W > U$,²⁹ the electronic properties of these mesoporous composites should depend strongly on the electronic configuration and oxidation state of the organometallic dopants, as well as the loading level and the interatomic spacing between the charge-carrier units, potentially influenced by the steric bulk of the supporting ligand system. While other factors such as surface conductivity and grain boundary effects may be at play, the dependence on electronic factors is readily illustrated by the dramatic difference in conductivity between *insulating* mixed oxidation state cobaltocene composites with a π^{*1}/π^{*0} configuration for Co(II) and Co(III), respectively, and the semiconducting bis(benzene)chromium composites with a configuration of $e_{2g}^4 a_{1g}^2 / e_{2g}^4 a_{1g}^1$ for Cr(0) and Cr(I), respectively.³⁰ In this case the much lower loading level of Cr (0.05–0.07 Cr:Nb ratio) in the niobium oxide mesostructure as compared to that of Co (0.3–0.5 Co:Nb ratio) in the analogous material would be expected to lead to lower conductivity in the Cr material, yet is obviously offset by the differences in relative electronic properties in the occluded species. It is thus anticipated that the changes in electron configuration, ionization potential, and electron affinity in this series of isostructural chromocene and vanadocene dopants will lead to composites with different electronic properties and that this change in electronic behavior may provide further insight into the nature of electron mobility in this new family of materials.

Experimental Method

Materials and Equipment. All chemicals unless otherwise stated were obtained from Aldrich. Samples of mesoporous niobium oxide (Nb-TMS1) were obtained from Alfa-Aesar and used without further purification. Trimethylsilyl chloride was obtained from Aldrich and distilled over calcium hydride.

(24) Murray, S.; Trudeau, M.; Antonelli, D. M. *Adv. Mater.* **2000**, *12*, 1339.

(25) Murray, S.; Trudeau, M.; Antonelli, D. M. *Inorg. Chem.* **2000**, *39*, 5901.

(26) Vettriano, M.; He, X.; Trudeau, M.; Antonelli, D. M. *J. Mater. Chem.* **2001**, *11*, 1.

(27) He, X.; Trudeau, M.; Antonelli, D. M. *Adv. Mater.* **2000**, *12*, 1036.

(28) He, X.; Trudeau, M.; Antonelli, D. M. Submitted for publication.

(29) Cox, P. A. *The Electronic Structure and Chemistry of Solids*; Oxford University Press: New York, 1987.

(30) Anderson, S. E., Jr.; Drago, R. S. *J. Am. Chem. Soc.* **1970**, *92*, 4244.

Nb-TMS1 samples were dried at 100 °C overnight under vacuum and then stirred with excess trimethylsilyl chloride in dry ether for 12 h under nitrogen. Nitrogen adsorption and desorption data were collected on a Micromeritics ASAP 2010. X-ray powder diffraction (XRD) patterns (Cu K α) were recorded in a sealed glass capillary on a Siemens D-500 $\theta/2\theta$ diffractometer. X-ray single-crystal data were collected on a Siemens SMART System CCD diffractometer, and the data sets were solved employing the SHELX-TL software package. All X-ray photoelectron spectroscopy (XPS) peaks were referenced to the carbon C-(C, H) peak at 284.8 eV, and the data were obtained using a Physical Electronics PHI-5500 XPS instrument using charge neutralization of 2–4 eV where appropriate. The conductivity measurements were recorded on a Jandel four-point universal probe head combined with a Jandel resistivity unit. The equations used for calculating the resistivity are as follows: for pellets of <0.1 mm thickness, $\rho = (\pi/\log n^2)(VI)t$

For pellets of >0.5 mm thickness, $\rho = 2\pi(S)(VI)$.

ρ = resistivity, $\pi/\log n^2$ = sheet resistivity, V = number of volts, I = current, t = thickness of the pellet, and S = the spacing of the probes (0.1 cm).

The powder UV-vis spectra were collected on an Ocean Optics S2000 fiber optics spectrometer equipped with an Analytical Instrument Systems light source emitter with a tungsten halogen lamp and an Ocean Optics UV 0.4 mm, 2 M reflection probe. The powder electron paramagnetic resonance (EPR) samples were prepared under vacuum and the data collected on a Bruker X-band ESP 300E EPR spectrometer. Magnetic measurements were conducted on a Quantum Design superconducting quantum interference device (SQUID) magnetometer MPMS system with a 5 T magnet. All elemental analysis data including inductively coupled plasma (ICP) were obtained from Galbraith Laboratories, 2323 Sycamore Dr., Knoxville, TN 37921-1700.

Synthesis. (a) To a suspension of trimethylsilylated Nb-TMS1 in dry benzene was added 1.5 mol of metallocene calculated on the basis of the molar percent Nb as determined by ICP. The mesoporous solid immediately went from a light faun color to a dark color. After several days of stirring to ensure complete absorption of the organometallic, the reduced material was collected by suction filtration and washed several times with benzene. Once synthesized, the material was dried in vacuo at 10^{-3} Torr on a Schlenk line until all condensable volatiles had been removed.

(b) Bis(cyclopentadienyl)vanadium ditriflate: A 0.15 g (0.0008 mol) sample of bis(cyclopentadienyl)vanadium in CH_2Cl_2 was added to a solution of 0.42 g (0.0016 mol) of AgSO_3CF_3 in CH_2Cl_2 with stirring under nitrogen. The color of the mixture immediately changed from purple to green. Stirring was continued for 1 h, and the solution was then filtered to remove the silver precipitate. The filtrate was evaporated to dryness, and the resulting solid was fully washed with benzene to give a dark solid. The crude product was recrystallized by vapor diffusion of ether into CH_2Cl_2 to afford the pure dication in 92% yield. The single-crystal structure of this vanadocene ditriflate compound is available as Supporting Information. Anal. Calcd for $\text{C}_{12}\text{H}_{10}\text{O}_6\text{F}_6\text{S}_2\text{V}$: C, 30.07; H, 2.10; V, 10.63; S, 13.38; F, 23.78. Found: C, 29.98; H, 2.03; V, 10.68; S, 13.47; F, 23.88.

(c) Bis(cyclopentadienyl)chromium triflate: The method to synthesize chromocenium triflate was similar to that above for vanadocenium ditriflate except a 1:1 molar ratio of chromocene and AgSO_3CF_3 was used. The total yield of this brown compound was 78%. Recrystallization of this compound in CH_2Cl_2 and ether gave brown needlelike crystals which were characterized by XPS, EPR, and UV. Anal. Calcd for $\text{C}_{11}\text{H}_{10}\text{O}_3\text{F}_3\text{SCr}$: C, 39.89; H, 3.04; Cr, 15.70; S, 9.68; F, 17.21. Found: C, 39.70; H, 2.83; Cr, 15.79; S, 9.81; F, 17.42.

Results

Since conductivity in molecular-based metals is strongly dependent on the ionization potential and

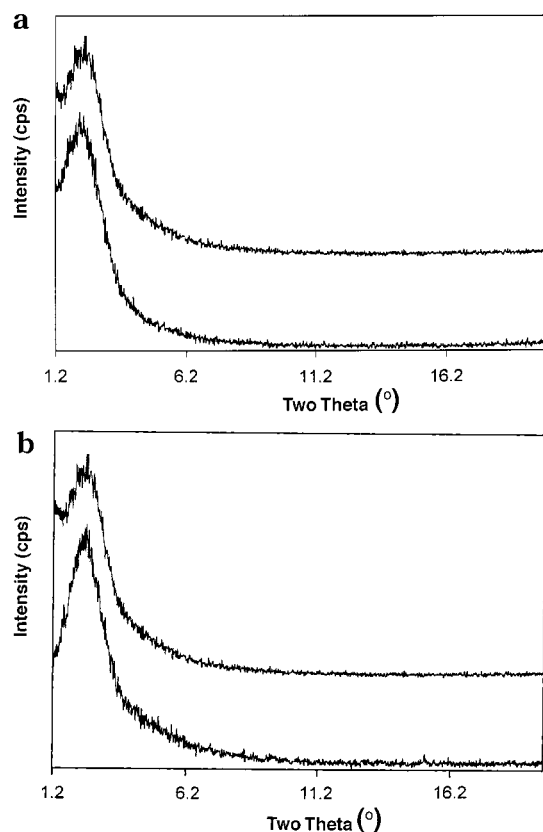


Figure 1. (a, top) XRD of mesoporous niobium oxide before (upper) and after (lower) treatment with excess bis(cyclopentadienyl)vanadium. (b, bottom) XRD of mesoporous niobium oxide before (upper) and after (lower) treatment with excess bis(cyclopentadienyl)chromium.

electron affinity of the species in question, and hence the electron configuration and oxidation state,³¹ we chose to investigate the changes in physical behavior of organometallic mesoporous niobium oxide composites on going from bis(benzene)vanadium(0), with a ground state of $e_{2g}^4 a_{1g}^1$, as a dopant to bis(cyclopentadienyl)vanadium(II), with a ground state of $e_{2g}^2 a_{1g}^1$. When a sample of trimethylsilated Nb-TMS1 with an XRD peak centered at $d = 38 \text{ \AA}$, an HK pore size of 24 \AA , a BET surface area of $712 \text{ m}^2 \text{ g}^{-1}$, and a pore volume of $0.470 \text{ cm}^3 \text{ g}^{-1}$ is treated with excess bis(cyclopentadienyl)vanadium in benzene over 2 days, a dark-colored material is formed which is collected by suction filtration and dried in vacuo for 6 h to ensure complete removal of free solvent from the structure. Figure 1a shows the XRD peak of the material after treatment with bis(cyclopentadienyl)vanadium. The peak centered at 38 \AA demonstrates that the material has fully retained its mesostructure on intercalation of the organometallic. Figure 2a shows the nitrogen adsorption and desorption isotherms of the materials from Figure 1a. The BET surface area of the treated sample dropped to $595 \text{ m}^2 \text{ g}^{-1}$, while the pore size and the pore volume decreased to 23 \AA and $0.282 \text{ cm}^3 \text{ g}^{-1}$, respectively. Figure 2c shows a plot of the HK pore size versus the incremental pore diameter before and after treatment. These data are

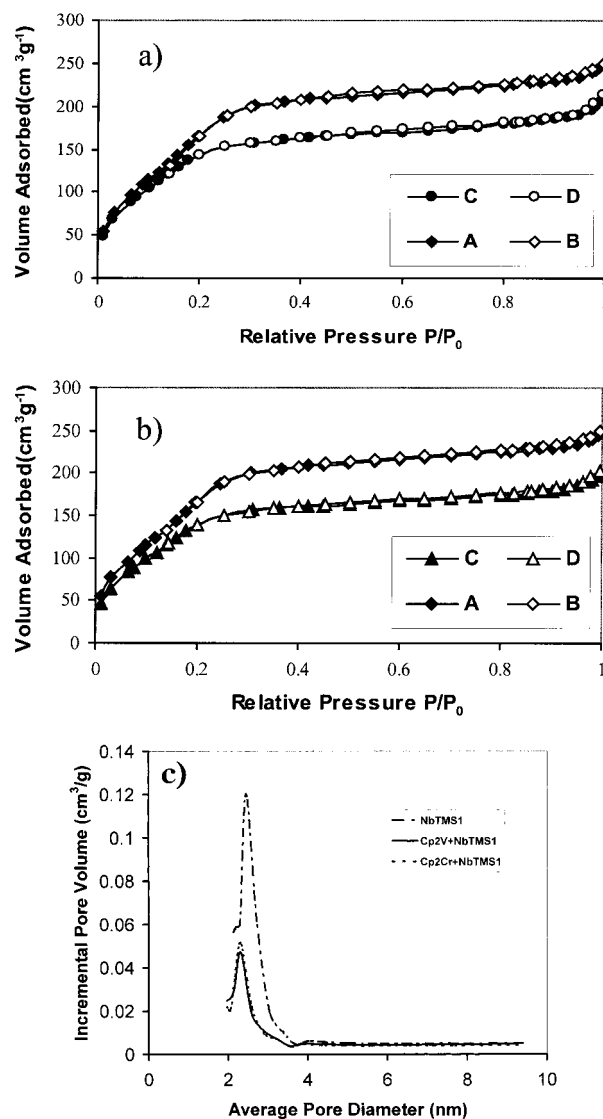


Figure 2. Nitrogen adsorption (A, C) and desorption (B, D) isotherms of mesoporous niobium oxide (a) before (A, B) and after (C, D) treatment with excess bis(cyclopentadienyl)vanadium and (b) before (A, B) and after (C, D) treatment with excess bis(cyclopentadienyl)chromium. (c) Incremental HK pore volume vs average pore diameter before (dashed line) and after treatment with excess bis(cyclopentadienyl)vanadium (solid line) or bis(cyclopentadienyl)chromium (dotted line).

consistent with partial occlusion of the pores of the mesostructure by the encapsulated organometallic. The elemental analysis of this new composite showed an increase in carbon from 4.65% in the starting material to values ranging from 9.07% to 9.87% depending on the sample. The increase in carbon is fully consistent with retention of the structure of the bis(cyclopentadienyl) complex without loss of the cyclopentadienyl rings. The V:Nb ratio in this material ranges from 0.10:1 to 0.15:1 as determined by ICP. This compares to other ratios in bis(benzene)vanadium-reduced composites of 0.3:1, and is consistent with the lower degree of reducing ability in the more highly oxidized organometallic.

The UV-vis spectrum of this material shows a complex series of absorbancies. The peak at 240 nm has been observed previously and can readily be assigned to the Nb-Osp VB-CB transition.⁶ The strong absorbancies at 214 and 298 nm are due to neutral bis-

(31) Almeida, M.; Gaudiello, J. G.; Kellogg, G. E.; Tetrick, S. M.; Marcy, H. O.; McCarthy, W. J.; Butler, J. C.; Kannewurf, C. R.; Marks, T. J. *J. Am. Chem. Soc.* **1989**, *111*, 5271.

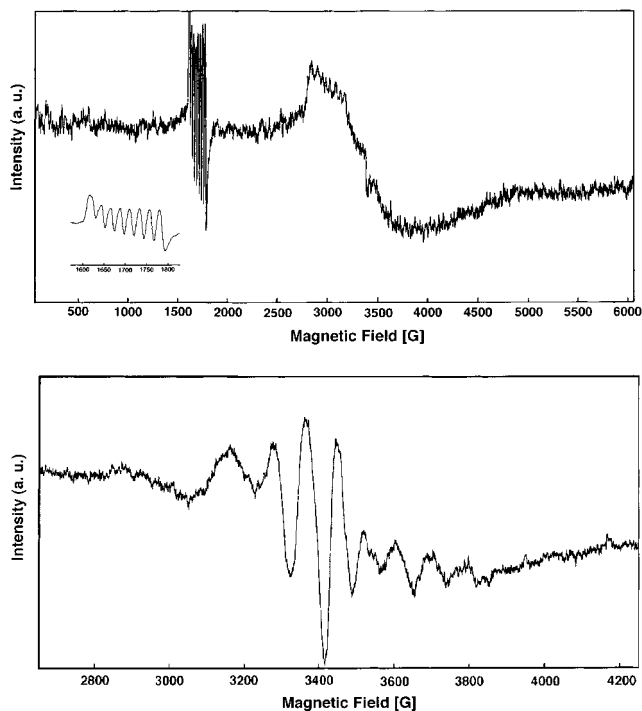


Figure 3. Powder EPR spectra of mesoporous niobium oxide treated with excess bis(cyclopentadienyl)vanadium in THF (a, top) at 77 K and (b, bottom) at room temperature with a V:Nb ratio of 0.005. The expansion is shown below to magnify the hyperfine splittings.

(cyclopentadienyl)vanadium,³² while that at 350 nm is due to a typical charge-transfer transition (LMCT) from the Cp ring to the V(IV) center in the bis(cyclopentadienyl)vanadium dication.³² The absorbance at ca. 580 nm appears in all reduced Nb-TMS1 species we have encountered to date and can be attributed to the Nb4d–Osp conduction band transition. These data confirm that bis(cyclopentadienyl)vanadium has been absorbed into the pore structure of the material and indicate that a portion of this species was oxidized by the niobium oxide framework as reported previously for the cobaltocene and bis(benzene)chromium intercalates.²⁴ While oxidation of bis(benzene)vanadium leads to formation of a monocation, the bis(cyclopentadienyl)vanadium cation is even more unstable to loss of an electron than neutral vanadocene species and thus loses a second electron to the mesostructure.³³

The EPR spectra of this material are shown in Figure 3. The powder sample was measured in THF at 77 K (Figure 3a). This spectrum shows two very well resolved sets of eight lines due to the ⁵¹V nucleus ($I = 7/2$). The first set of eight lines at 3000 G affords $g_{\parallel} = 2.26$ and an average hyperfine splitting of $A = 47.3$ G, originating from the resonance of the main rotation axis (z -axis) of the neutral bis(cyclopentadienyl)vanadium molecule oriented along the magnetic field. The second set of stronger eight lines at almost half-field (1700 G) gives $g_{\perp} = 4.00$ and an average hyperfine splitting of $A = 23.4$ G due to the bis(cyclopentadienyl)vanadium rotation axis being perpendicular to the magnetic field.³⁴ The broad peak at 3386.9 G ($g = 2.00$) can be assigned to

the free electron in the reduced mesostructure and appears in the EPR spectra of all reduced mesoporous niobium oxide materials we have studied to date.²⁸ Figure 3b shows the room-temperature powder spectrum of this material at a V:Nb ratio of 0.005 (equiv/equiv). The lower level of V was required to prevent spin–spin interactions between the organometallics at the higher ratio to observe hyperfine splittings. The very well resolved eight lines are also due to the ⁵¹V nucleus ($I = 7/2$). The asymmetry of this spectrum suggests both the g factor (average $g = 2.02$) and the hyperfine interactions (an average hyperfine splitting of $A = 90.3$ G) are anisotropic. The larger hyperfine splitting of the bis(cyclopentadienyl)vanadium dication in this material as compared to that in the solvent ($A = 75$ G) is due to Jahn–Teller distortion to the ²E_{2g} state in the reduced mesopores.³⁵ These data confirm the presence of the bis(cyclopentadienyl)vanadium dication in the sample, and are consistent with the mixed oxidation state formulation of this material where one-dimensional wires or agglomerates of bis(cyclopentadienyl)vanadium and its corresponding dication reside in the pores of a partially reduced niobium oxide framework.

To further investigate the composition and electronic structure of this new material, XPS studies were conducted. Figure 4a shows the Nb 3d region with the 5/2 and 3/2 peaks in clear evidence. The positions of the 3/2 and 5/2 peaks at 210.1 and 207.3 eV, respectively, are consistent with reduction of the Nb by roughly 1/10 of an oxidation state as compared to previous work.⁶ These emissions are also broader than those in the starting material, as is the O 1s peak, providing further evidence for reduction of the Nb framework by bis(cyclopentadienyl)vanadium. Figure 4b shows the V 2p 3/2 and 1/2 regions of the spectrum and displays a series of emissions which can be simulated to fit a mixture of the neutral bis(cyclopentadienyl)vanadium species (513.0 and 520.2 eV), a vanadium(IV) species (514.9 and 522.4 eV), and a V(V) species (516.4 and 524.5 eV).³⁶ XPS simulations give a ratio among these three species of 1:14:6. The much smaller peak of the neutral bis(cyclopentadienyl)vanadium species may be due to vaporization under the high-vacuum conditions of the XPS experiment.³⁷ To confirm the nature of the vanadium(IV) species, vanadocinium ditriflate was synthesized by treatment of vanadocene with silver triflate. The XPS spectrum of this previously unknown compound shows emissions in the V 2p 3/2 and 1/2 regions at 514.8 and 522.3 eV (Figure 4c), completely consistent with the V(IV) emissions in the spectrum from Figure 4b. Figure 4d shows the region near the Fermi level of the XPS spectrum of the composite with a rough distance to the Fermi level of ca. 3.0 eV for the metal–oxygen sp valence emission, comparable to that observed in related materials.²⁴ The conductivity of these composites is $10^{-5} \Omega^{-1} \text{cm}^{-1}$, lower than that obtained for the bis(benzene)vanadium composites of $10^{-4} \Omega^{-1} \text{cm}^{-1}$.

(34) McConnell, H. M.; Porterfield, W. W.; Robertson, R. E. *J. Chem. Phys.* **1959**, *30*, 442; Prins, R.; Biloen, P.; van Voorst, J. D. W. *J. Chem. Phys.* **1967**, *46*, 1216.

(35) Armstrong, D. R.; Fortune, R.; Perkins, P. G. *J. Organomet. Chem.* **1976**, *111*, 197.

(36) *Handbook of X-ray Photoelectron Spectroscopy*; Physical Electronics Division, Perkin-Elmer Corp.: Eden Prairie, MN.

(37) Pure samples of bis(cyclopentadienyl)vanadium and -chromium sublime readily under the conditions of the XPS experiments.

(32) Gordon, K. R.; Warren, K. D. *Inorg. Chem.* **1978**, *17*, 987.

(33) Green, J. C.; Payne, M. P.; Teuben, J. H. *Organometallics* **1983**, *2*, 203.

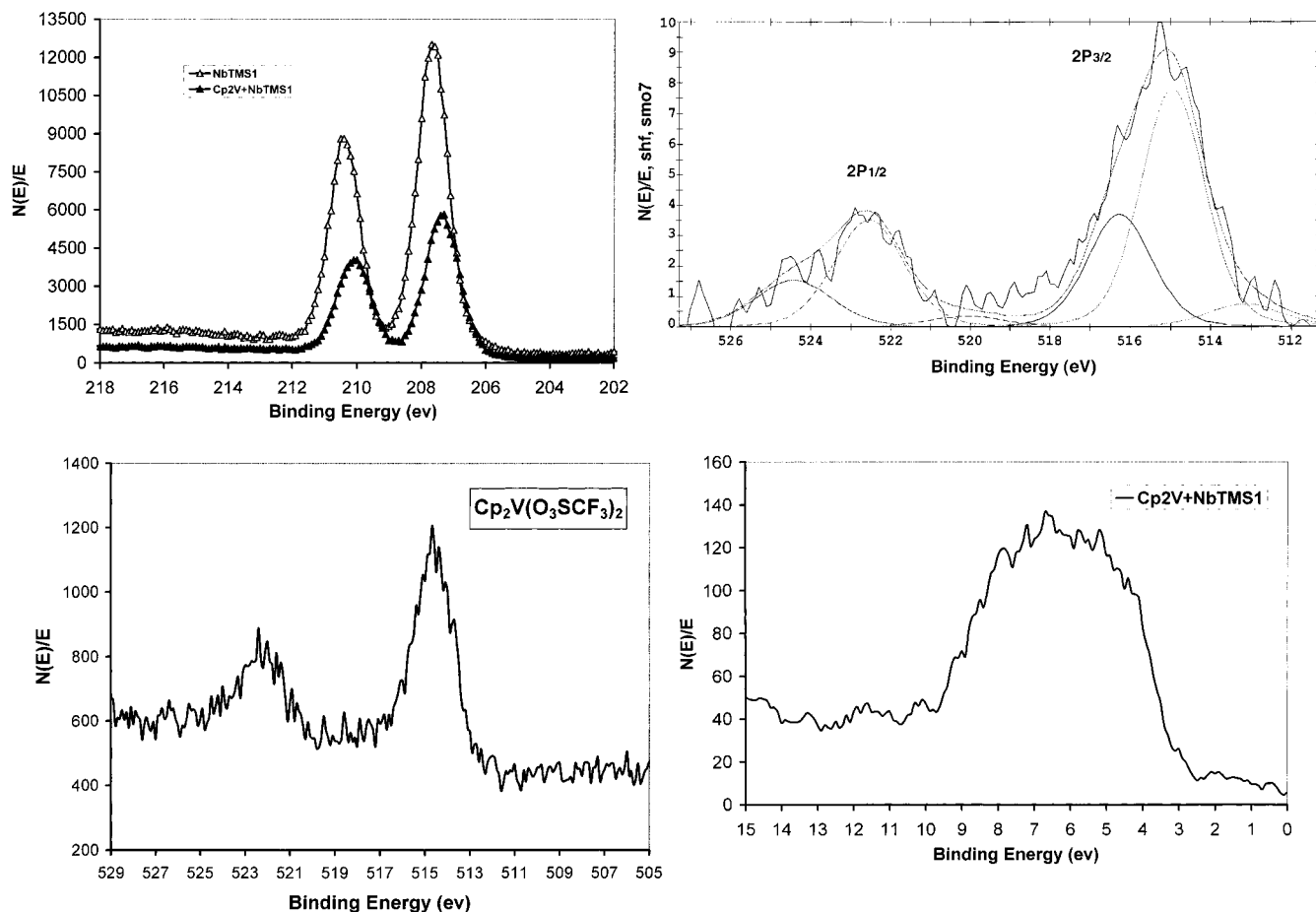


Figure 4. XPS spectra of mesoporous niobium oxide treated with excess bis(cyclopentadienyl) vanadium showing the (a, top left) Nb 3d 3/2 and 5/2 regions, (b, top right) V 2p 1/2 and 3/2 regions and (c, bottom left) V 2p 1/2 and 3/2 regions of vanadocenium ditrflate, and (d, bottom right) region near the Fermi level.

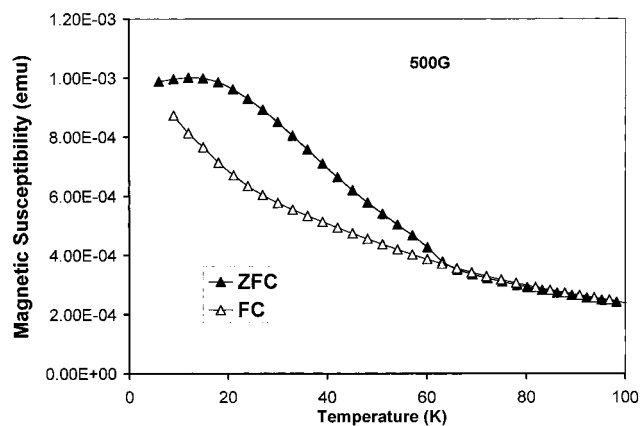


Figure 5. SQUID magnetometer plot of magnetic susceptibility per gram versus temperature (M vs T) for a sample of mesoporous niobium oxide treated with excess bis(cyclopentadienyl)vanadium showing the field-cooled (FC) and zero-field-cooled (ZFC) branches of the plot.

Figure 5 shows the SQUID magnetometer plot of magnetic susceptibility versus temperature for the composite, indicating that this material is paramagnetic. This is expected from the presence of unpaired electrons in the structure. The hysteresis in this curve can be attributed to the broad distribution of particle sizes in the mesoporous oxide, with a wide range of roughly spherical particles from 50 to 1000 nm as

previously determined by scanning electron microscopy (SEM).²³ The slight transition in the ZFC branch of the plot possibly indicates some degree of superparamagnetism or spin glass behavior at low temperature, although this contribution is clearly much weaker than observed for related nickelocene intercalates.²⁶ The B vs H plots at 5 and 100 K of this material are linear, typical only of paramagnetic species, demonstrating that superparamagnetic or spin glass contributions do not dominate the magnetic behavior in this system.

To further probe into the effect of changing from a neutral bis(benzene) complex to its corresponding bis(cyclopentadienyl) complex, the bis(cyclopentadienyl)-chromium intercalates were synthesized. Because this complex has an electronic ground-state configuration of $e_{2g}^3 a_{1g}^1$, different from that of the neutral bis(benzene)-chromium(0) species ($e_{2g}^4 a_{1g}^2$), different electronic properties for the corresponding mesoporous niobium oxide composites were anticipated. Thus, treatment of a sample of trimethylsilated mesoporous niobium oxide with a BET surface area of $712 \text{ m}^2 \text{ g}^{-1}$, an HK pore size maximum at 24 \AA , and an XRD pattern with a single peak at $d = 38 \text{ \AA}$ with excess bis(cyclopentadienyl)-chromium(II) in benzene at ambient temperature for 2 days gave a new dark green to gray material which was isolated by suction filtration and washed repeatedly with benzene followed by drying in vacuo at 10^{-3} Torr. The XRD pattern of this new material is shown in Figure 1b and displays a peak at $d = 38 \text{ \AA}$, indicating

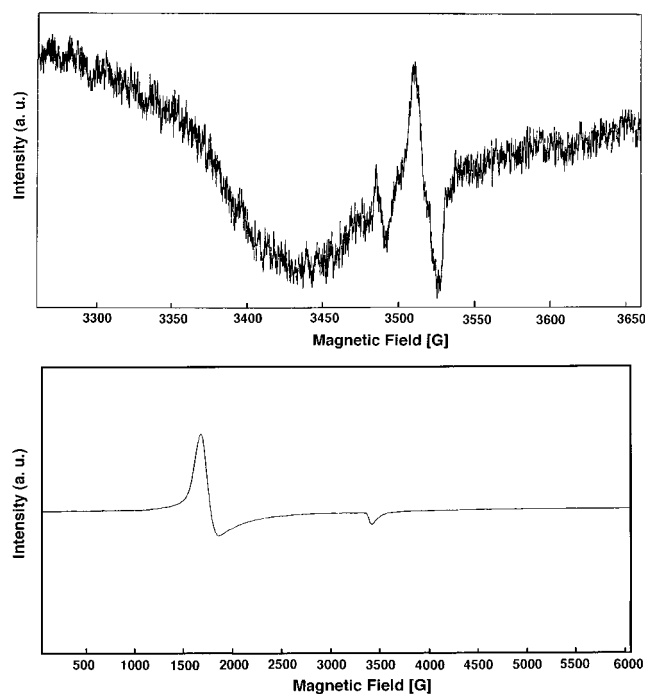


Figure 6. Powder EPR spectra of mesoporous niobium oxide treated with excess bis(cyclopentadienyl)chromium in THF (a, top) at room temperature and (b, bottom) at 77 K.

that the mesostructure has been fully retained. The nitrogen adsorption-desorption isotherms of the starting material and bis(cyclopentadienyl)chromium composite are shown in Figure 2b. The BET surface area of the composite is $589 \text{ m}^2 \text{ g}^{-1}$ with an HK pore size maximum at 23 \AA . Figure 2c shows a plot of the HK incremental pore volume versus the average pore diameter. The pore volume of this material dropped from 0.470 to $0.287 \text{ cm}^3 \text{ g}^{-1}$. All of these data confirm retention of the mesostructure with partial occlusion of the pores with one or more organometallic chromium species. Elemental analysis of this new material gave values of $9.23\text{--}9.74\%$ C and a molar ratio of Cr:Nb of $0.10\text{--}0.13:1$. The UV-vis reflectance spectrum showed a broad range of absorbances from 250 to 800 nm with peaks at 225 and 332 nm corresponding to the neutral chromium species and a peak at 280 nm which can be assigned to the cation as compared to the UV spectra of bis(cyclopentadienyl)chromium triflate and previous work conducted on the chloride salt of this cation.^{38b} The EPR spectra of this material are shown in Figure 6a,b. The powder spectrum of this material shows evidence for a three-electron system ($S = 3/2$), most likely the bis(cyclopentadienyl)chromium cation, present in these materials. The two lines in Figure 6b are due to the anisotropy of the g factor, which gives two g values, i.e., $g_{\parallel} = 1.98$ and $g_{\perp} = 3.98$, according to the simulation of this spectrum. The much larger peak at g_{\perp} than that at g_{\parallel} indicates a very large number of bis(cyclopentadienyl)chromium cations with axes nearly perpendicular to the magnetic field direction. Also, both of these lines come from the transition $\langle +1/2 \rangle \leftrightarrow \langle -1/2 \rangle$. The other two transitions $\langle \pm 1/2 \rangle \leftrightarrow \langle \pm 3/2 \rangle$, which are allowed by selection rules, are not detectable because of the very large zero-field interaction (D value). This case often

occurs in a Cr(III) system, and can be readily fitted to an $S = 1/2$ spin Hamiltonian of the form $H = \beta_e [g_{\perp} (B_x S_x + B_y S_y) + g_{\parallel} B_z S_z]$, but $g_{\perp} = (S + 1/2)g'_{\perp}$, where g'_{\perp} is the value in the regular S spin Hamiltonian (often close to 2). Solid samples of bis(cyclopentadienyl)chromium did not show any signal at room temperature or low temperature as described previously for this complex;³⁹ however, the spectrum of this species was obtained by observing the powder sample in THF at room temperature (Figure 6a). The two lines in this spectrum at 3517 G ($g = 1.988$) and 3488 G ($g = 2.00$) are consistent with a triplet ground state ($S = 1$) of neutral bis(cyclopentadienyl)chromium due to the transitions $\langle \pm 1 | \leftrightarrow \langle 0 |$. The half-field transition $\langle +1 | \leftrightarrow \langle -1 |$ was too weak to be resolved because of unfavorable selection rules for this transition.⁴⁰

The Cr 2p $1/2$ and $3/2$ regions of the X-ray photoelectron (XPS) spectrum of the mesoporous composite and its simulation are shown in Figure 7a. This spectrum exhibits emissions at 584.5 and 574.8 eV and 585.5 and 575.7 eV corresponding to neutral bis(cyclopentadienyl)chromium³⁶ and a Cr(III) species, respectively. The other peaks at 587.1 and 577.4 eV can be assigned to a higher oxidation state Cr(IV) species. The integrated intensity ratio of these three peaks was calculated as $1:6:6$, respectively. The lower intensities of the emissions due to neutral bis(cyclopentadienyl)chromium relative to the other species are possibly due to vaporization effects as seen for the vanadium analogue. To confirm that the Cr(III) emissions were due to the presence of the bis(cyclopentadienyl)chromium cation in the pores, we synthesized chromocenium triflate. The XPS spectrum of this brown compound (shown in Figure 7b) gives the Cr 2p $1/2$ and $3/2$ regions at 585.5 and 575.8 eV , virtually identical with the emissions for the Cr(III) species present in the composite at higher binding energy. The Nb 3d region of the XPS (Figure 7c) shows $5/2$ and $3/2$ peaks at 207.2 and 210.0 eV , demonstrating that the walls of the mesostructure are only slightly reduced in this material compared to the starting material, which shows emissions at 207.8 and 210.6 eV .³ These data are consistent with a small degree of electron transfer into the walls of the mesostructure and formation of the bis(cyclopentadienyl)chromium cation and other more highly oxidized species. The valence region near the Fermi level (Figure 7d) shows a broad and complex hump for the Nb-O sp valence emission with a tail that ends at roughly 3.0 eV , consistent with other mesoporous niobium oxide composites studied.³ The conductivity measurements showed that this material is semiconducting with a value of $10^{-6} \Omega^{-1} \text{ cm}^{-1}$, which compares to those of the mesoporous niobium oxide composites of other early-transition-metal sandwich compounds such as bis(benzene)vanadium, bis(benzene)chromium, and bis(cyclopentadienyl)vanadium.

SQUID magnetic measurements were conducted to further explore the magnetic behavior of this new composite. The M vs T plot measured at 500 G is shown in Figure 8 and provides evidence for paramagnetic and possibly spin glass or superparamagnetic behavior of this material. The B vs H plot for this material run from 100 to 5 K gives a straight line with very small

(38) (a) Ghosh, P.; Kotchevar, A. T. *Inorg. Chem.* **1999**, *38*, 3730.
(b) Ozin, G. A.; Godber, J. J. *Phys. Chem.* **1989**, *93*, 878.

(39) Barrera, J. A.; Wilcox, D. E. *Inorg. Chem.* **1992**, *31*, 1745.
(40) Desai, V. P.; Konig, E. *J. Chem. Phys.* **1983**, *78*, 6299.

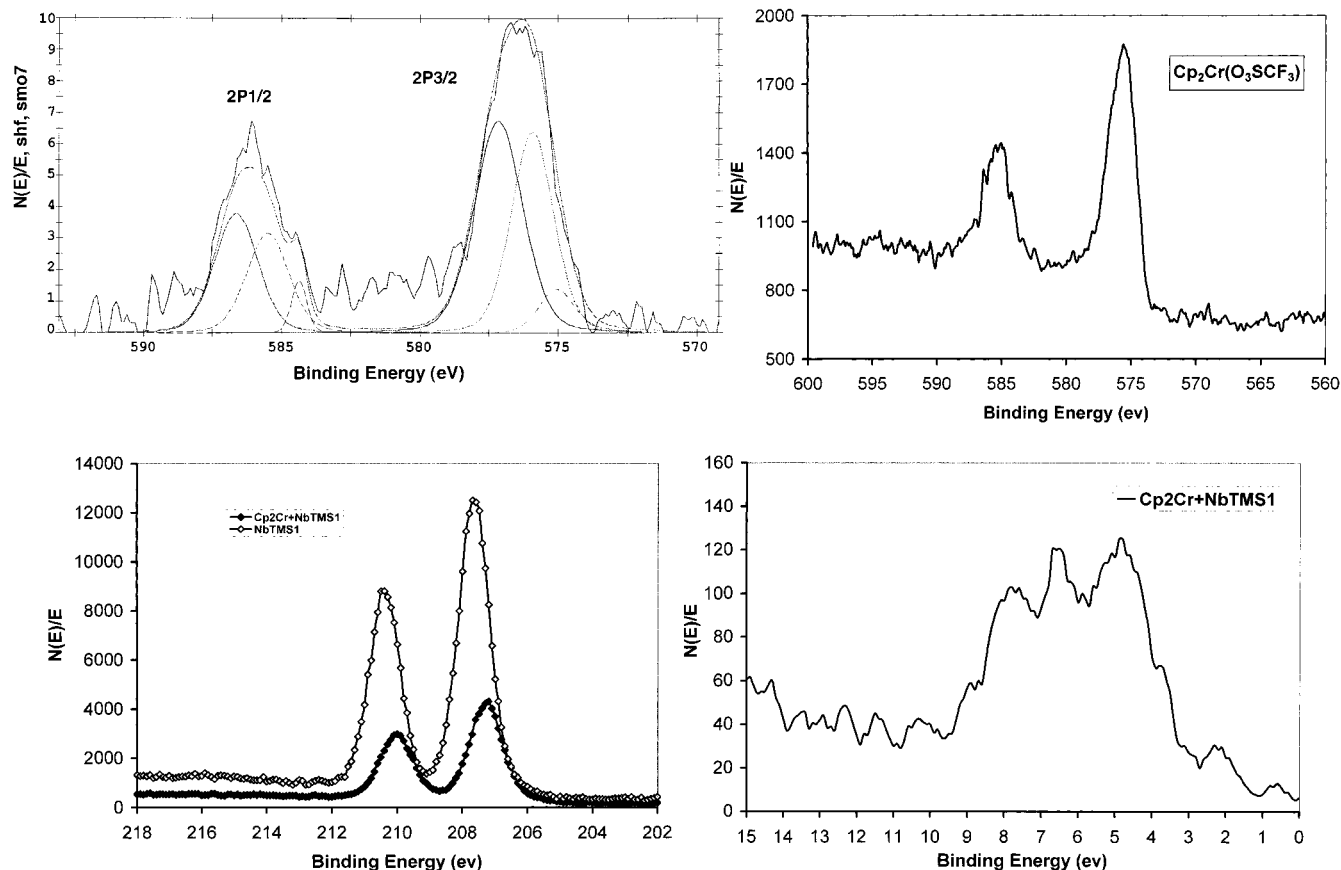


Figure 7. XPS spectra of mesoporous niobium oxide treated with excess bis(cyclopentadienyl)chromium showing the (a, top left) Cr 2p 1/2 and 3/2 regions and (b, top right) Cr 2p 1/2 and 3/2 regions of chromocenium triflate, (c, bottom left) Nb 3d 3/2 and 5/2 regions, and (d, bottom right) region near the Fermi level.

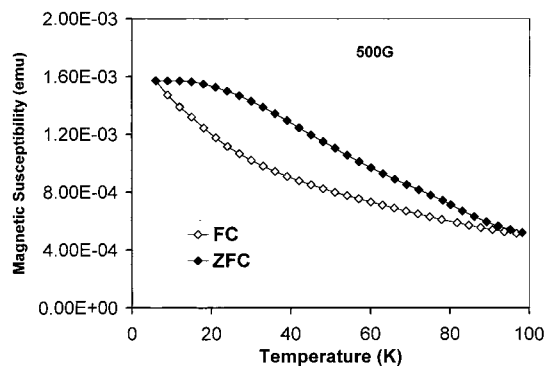


Figure 8. SQUID magnetometer plot of magnetic susceptibility per gram versus temperature (M vs T) for a sample of mesoporous niobium oxide treated with excess bis(cyclopentadienyl)chromium showing the FC and ZFC branches of the plot.

hysteresis, demonstrating that the paramagnetic contribution dominates the magnetic behavior of the system. The large hysteresis in Figure 8 can also be explained by a wide particle size distribution or a slight transition in the ZFC branch of the plot near 20 K indicative of superparamagnetic or spin glass behavior. These two factors have been clearly shown by reduced two-membered NbV mesoporous materials in our group.

Discussion

In light of the insulating nature of mesoporous niobium oxide reduced with alkali metals, the conduc-

tivity trends in these materials are best explained by a model in which the charge carrier involves the organometallic phase in the pores or on the surface of the material. Since treatment of amorphous nonporous samples of niobium oxide, of average particle size similar to that of the mesoporous niobium oxide used in this study as judged by SEM, with bis(cyclopentadienyl) complexes of Cr and V leads to reduced materials with XPS spectra similar to those of the respective mesoporous composites but much lower conductivity (ca. $10^{-8} \Omega^{-1} \text{cm}^{-1}$), it can be argued that the surface contribution to conductivity is negligible. Unpublished results in our group have demonstrated that samples of mesoporous niobium oxide prepared with 5 molar % vanadium in the walls are insulating as are those same materials reduced with up to 1 equiv of potassium naphthalene. This suggests that the role of higher oxidation state V residues in the structure in conductivity is also negligible and that any reduced vanadium in the walls is not important in the overall conductivity of these materials. Thus, conductivity in these composites is best attributed to mixed oxidation state V(II)/V(IV) or Cr(II)/Cr(III) chains in the pores, which act as pseudo-one-dimensional molecular wires where the hole induced by oxidation of a portion of the organometallic by the framework is likely the charge carrier. In previous work we found that the presence of the neutral species in the pores for bis(benzene)vanadium and -chromium composites of mesoporous niobium oxide was required for conductivity.²⁴ This rules out any conductivity mechanism involving only the reduced mesostructure and the

organometallic cation. While assignment of any discrete local structure to the organometallic phase within the pores is premature, further spectroscopic studies are ongoing to determine average intermolecular distances and orientations in the pores of the species in question. The distance between adjacent units is expected to be critical in such a model, as it is in the conductivity of one-dimensional Pt chains; however, at room temperature there is likely enough thermal energy to allow enough motion of these individual units such that constant proximity is not a requirement and thermally induced collisions can facilitate electron mobility. This is certainly the case in most molecular metals, which possess high enough thermal vibration energy at room temperature to overcome charge density waves and Peierl's distortion, which tend to cause electron localization and insulating behavior below a certain temperature threshold.²⁹ The role of oxidation state and electron configuration is less clear; however, the dramatic difference in conductivity between cobaltocene-loaded mixed oxidation state materials with 0.5 equiv of Co (sum of Co(II) and Co(III)) and the materials under study suggest that the electronic nature of the charge carriers is more important than the absolute loading percent of the organometallic dopant.

Since conductivity in solids depends on the Hubbard potential ($U = I - A$), where I is the ionization potential and A is the electron affinity of the charge-carrying species, and the bandwidth (W), quantifying these parameters in the systems under study may be helpful in understanding the trends in electronic behavior. If W is greater than U , the material will be conducting; if it is not, then the material will be insulating. The Hubbard potential can be estimated by considering the literature I values of 6.78 and 5.71 eV for bis(cyclopentadienyl)vanadium and -chromium, respectively,⁴¹ along with the A values for the respective cationic species. Although the latter are not available in the literature, they can be estimated from the A values for the neutral organometallic species and the corresponding oxides. The A values for V(II)O and V(IV)O₂ are 1.23 eV⁴² and 2.01 eV,⁴³ respectively, while that for bis(cyclopentadienyl)vanadium (II) is 0.68 eV.⁴⁴ Since the value for V(II)O is higher than that of bis(cyclopentadienyl)vanadium (II), the cyclopentadienyl ligand environment alters the A value with respect to the O ligand environment by $1.23 - 0.68 = 0.55$ eV. From this we can estimate the A value for the bis(cyclopentadienyl)vanadium (IV) dication as $2.01 - 0.55 = 1.46$ eV. Likewise, considering the values of 0.88, 1.22, and 2.41 eV for the electron affinities of bis(cyclopentadienyl)-chromium(II),⁴⁴ Cr(II)O,⁴² and Cr(IV)O₂,⁴³ respectively (a reliable value for the A of Cr₂(III)O₃ is not available), and using half the difference between Cr(II)O and Cr(IV)O₂, we can arrive at an estimation of 1.47 eV for the A of the bis(cyclopentadienyl)chromium(III) cation. Thus, U for the V system can be estimated as

$6.78 - 1.39 = 5.39$ eV, while that for the Cr system can be estimated as $5.71 - 1.47 = 4.24$ eV. While W is difficult to calculate in an amorphous composite system, comparisons to values for the elements may still be helpful in the systems under study, since all other factors such as cyclopentadienyl ligand environment, organometallic loading level, and temperature (influencing thermal motion and charge-carrier collision frequency) are roughly equal. From the estimated U calculated above and the bandwidth W of 6.77 eV for V and 6.56 eV for Cr calculated assuming a body-centered cubic structure,⁴⁵ it would appear that conductivity in both systems should be favorable due to the 1.38 and 2.32 eV values for $W - U$ for the V and Cr systems, respectively.

Applying this model to the cobaltocene materials is valuable in understanding the origin of conductivity in this family of composites, since these materials possess a much higher loading level than the V and Cr systems by almost a factor of 50, yet are still insulating. The Hubbard potential U can be calculated from an I of 5.56 eV⁴¹ for cobaltocene and an A estimated from the sum of the A value for cobaltocene and half the difference between the A value for Co(II)O⁴² and Co(IV)O,⁴³ given that the literature A value for Co₂(III)O₃ is not available. This gives a value of 4.30 eV for U , while W for Co is 4.35 eV.⁴⁵ The difference between U and W of 0.05 eV is almost negligible and would thus be expected to lead to a much more insulating material than the Cr and V systems, which have much larger and more favorable values for $W - U$ of 1.38 and 2.32 eV, respectively. It thus appears that the governing factor in conductivity in this system is likely the balance between U and the bandwidth W of the transition metal in question, which is known to decrease monotonically across a table due to an increase in effective nuclear charge. This explanation is commonly invoked to explain the conductivity trends of simple monoxides from TiO to CoO across the periodic table.⁴⁵ However, owing to the amorphous nature of the material as well as the potential degree of state crossing and orbital mixing between the a and e levels of the metallocene systems, specific band assignments for these materials are as yet ambiguous.

Conclusion

In summary, treatment of mesoporous niobium oxide with bis(cyclopentadienyl)vanadium and -chromium led to materials with pseudo-one-dimensional mixed oxidation state metallocene wires in the pore structure. The specific nature of the species present was confirmed by EPR, UV, and XPS to show that the structural integrity of the organometallic was retained after electron transfer to the niobium oxide framework. The conductivity in these materials was attributed to the oxidation-induced hole in the organometallic phase in light of the fact that all samples of alkali-metal-reduced mesoporous niobium oxide are insulating. The trends in conductivity from V and Cr to Co fit well into the model predicted from considering estimated bandwidths and the Hubbard potential. We are currently conducting further

(41) Evans, S.; Green, M. L. H.; Jewitt, B.; King, G. H.; Orchard, A. F. *J. Chem. Soc., Faraday Trans. 2* **1974**, *70*, 356.

(42) Gutsev, G. L.; Rao, B. K.; Jena, P. *J. Phys. Chem. A* **2000**, *104*, 5374.

(43) Gutsev, G. L.; Rao, B. K.; Jena, P. *J. Phys. Chem. A* **2000**, *104*, 11961.

(44) Giordan, J. C.; Moore, J. H.; Tossell, J. A.; Weber, J. *J. Am. Chem. Soc.* **1983**, *105*, 3431.

(45) Harrison, W. A. *Electronic Structure and the Properties of Solids*; Dover Publications: New York, 1989.

spectroscopic studies to determine the interatomic distances and orientations of the intercalated phase.

Acknowledgment. Financial support of this research by the National Science and Engineering Research Council of Canada (NSERC) and Ontario Premier's Research Excellence Award is acknowledged. We are also grateful to Dr. Bruce McGarvey for his help with the EPR spectrum. Dr. D. Stephan and Dr. P. Wei

are thanked for their help with the X-ray crystallography.

Supporting Information Available: ORTEP diagram of the dark green single crystal of vanadocesium ditriflate obtained by vapor diffusion methods (PDF). This material is available free of charge via the Internet at <http://pubs.acs.org>.

CM0104102